Direct Power Control for Dual-Active-Bridge Converter

NGUYEN Duy Dinh and FUJITA Goro

Graduate School of Engineering and Science, Shibaura Institute of Technology
Email: na14503@shibaura-it.ac.jp

***Abstract*—This paper proposes a new strategy to control a single-phase frequency-modulated Dual-Active-Bridge (DAB) converter. Since the active and reactive power at one side of the isolated transformer are proportional to the direct and quadrature current components, I_d and I_q, decoupling control of the two current components can help managing the power directly. A linear observer is designed to detach I_d and I_q from the transferred current. By applying an appropriate pairing strategy, the interaction between d- and q-axis is negligible and a decoupling control algorithm is able to be applied. A laboratory-scaled experiment system of 250W DAB converter has been built to evaluate the proposed control algorithm. A TI-TMS320F28335 control card is employed for PWM generation, meanwhile a dSPACE 1103 system is utilized to accomplish the control strategy. Experiment results show that, the proposed control strategy requires not very high sampling frequency but provides observed currents $\hat{I}_d$ and $\hat{I}_q$ with acceptable accuracy. The outcome of this paper allows to use a low-cost DSP platform to handle the active and reactive power within a high-frequency DAB converter individually.**

I. Introduction

Dual-active-bridge (DAB) converter is first introduced by De Doncker *et. al.* [1] in 1991. Since then, it has played a very important role in many applications such as solid state transformer [2], energy storage system of electric vehicle [3], or aerospace [4], etc. Several major advantages of DAB converter can be listed as: bidirectional power transmission; galvanic isolation and high voltage ratio can be achieved due to the use of a high frequency transformer; and space saving because the leakage inductance of the transformer can be utilized as the power transmission container.

Conventionally, in order to control a single-phase DAB converter, one loop voltage mode [2], [5] is applied. In [6], a strategy basing on feed-forward load current in conjunction with the voltage loop was represented. Two loops current mode topology was introduced in [3], however, the controlled variable is the DC output current. In term of dynamic control for multi-phase DAB converter, a strategy in stationary $\alpha\beta$-frame was presented in [7]. In [8], a control system based on dq-rotation coordinator was addressed. In that system, a dq-transformation was employed to separate two current components, I_d and I_q. In the aforementioned publications, only active power is regulated, none of them manages the circulating (reactive) power within the inverters.

The scope of this paper is dynamic control of a single-phase-frequency-modulated DAB converter intended to be applied in DC transmission application. The target is to control the active and reactive power individually. As seen later in section II, it can be done by decoupled control of the direct and quadrature current components detached from the transfered current. Since the converter is single phase typed, the transferred current is single phase as well. If the frequency is relatively low, its instantaneous value can be sampled with a high speed DSP platform. After that, an orthogonal signal can be generated from the measured one before leading the two signals into a coordinate transformation. A single phase PLL should be employed to provide the synchronize signal for the transformation [9]. This method requires a very high sampling speed and high calculation performance of the DSP. If the switching frequency is high, the resolution of the feedback signal may not enough for high accuracy control.

In this paper, an observer is designed to estimate the two current components from the average absolute transferred current. After that, a simple decoupling strategy is utilized to reduce the interaction between the two control channels. Two simple PI controllers are synthesized to complete the decoupling control system. The construction of this paper is as followed: the mathematic equations describing the converter are derived in section II; design of the observer and decoupling technique are addressed in section III; finally, the simulation and experiment results demonstrated in section IV will confirm the validity of the proposed control strategy.

II. State state analysis

The DAB converter is depicted in Fig. 1. Two H-bridge inverters are located at the primary and the secondary sides of a high-frequency transformer with the ratio of $n:1$. The input DC voltage of the primary and secondary inverters are V_1 and V_2, respectively. The power electronic devices S_{1-4} and T_{1-4} can be either MOSFET or IGBT. Both H-bridges operate in 180 degrees conduction mode. There is a bridge shift angle ψ between the two inverters to handle the power flow. For simplification, the primary referred equivalent circuit of the converter expressed in Fig. 2 is utilized in the analysis. The fundamental component of the voltages across the primary and secondary winding of the transformer are denoted as V_{1e} and V'_{2e}, respectively; the first harmonic component of the transferred current is I_e; R_s and L_s are the equivalent primary referred resistance and inductance of the transferred path. Since both inverters are modulated with the same switching

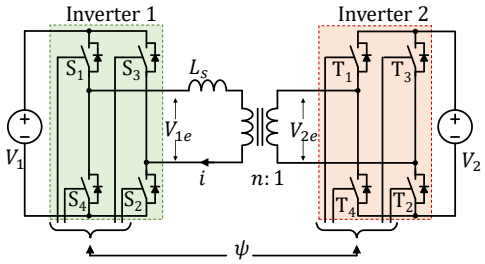

Fig. 1: Isolated-dual-active-bridge converter.

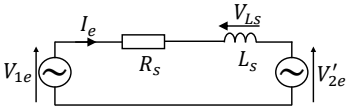

Fig. 2: Primary referred equivalent circuit.

frequency f_s, the output voltages and the transferred current can be seen as rotation vectors $\vec{V}_{1e}, \vec{V}'_{2e}$, and $\vec{I}_e$ with the same angular speed of ω_s ($\omega_s = 2\pi f_s$). The projection of $\vec{V}_{1e}, \vec{V}'_{2e}$, and $\vec{I}_e$ on d- and q-axis of a dq-frame rotating synchronously with and being aligned along $\vec{V}_{1e}$ will be DC components. A vector diagram demonstrating the relationship of those vectors is depicted in Fig. 3. According to [10], the voltage and current vectors can be represented as:

$$\vec{V}_{1e} = \begin{bmatrix} V_{1d} \\ V_{1q} \end{bmatrix} = \frac{4}{\pi} \begin{bmatrix} V_1 \\ 0 \end{bmatrix} \tag{1}$$

$$\vec{V}'_{2e} = \begin{bmatrix} V_{2d} \\ V_{2q} \end{bmatrix} = \frac{4}{\pi} \begin{bmatrix} nV_2 \cos\psi \\ nV_2 \sin\psi \end{bmatrix} \tag{2}$$

$$\vec{I}_e = \begin{bmatrix} I_d \\ I_q \end{bmatrix} = K_I \begin{bmatrix} (M - \cos\psi) + F_x Q_{L0} \sin\psi \\ F_x Q_{L0} (M - \cos\psi) - \sin\psi \end{bmatrix} \tag{3}$$

where V_{1d}, V_{1q}, V_{2d}, V_{2q}, I_d and I_q are the d- and q-components of the corresponding voltage and current vectors; Q_{L0} is the quality factor of the equivalent inductor L_s at the nominal switching frequency, $Q_{L0} = \dfrac{\Omega_s L_s}{R_s}$, Ω_s is the nominal switching frequency; F_x is the frequency modulation factor, $F_x = \dfrac{\omega_s}{\Omega_s}$; M is the voltage ratio between the two terminals, $M = \dfrac{V_1}{nV_2}$; and $K_I = \dfrac{4nV_2}{\pi R_s} \times \dfrac{1}{1 + F_x^2 Q_{L0}^2}$.

From (1), (2) and (3), the instantaneous active and reactive power can be calculated by (4) and (5):

$$\begin{bmatrix} P_1 \\ Q_1 \end{bmatrix} = \frac{1}{2} \begin{bmatrix} V_{1d} I_d \\ V_{1d} I_q \end{bmatrix} = K_P \begin{bmatrix} \sin\psi + \dfrac{M - \cos\psi}{F_x Q_{L0}} \\ (M - \cos\psi) - \dfrac{\sin\psi}{F_x Q_{L0}} \end{bmatrix} \tag{4}$$

$$\begin{aligned} \begin{bmatrix} P_2 \\ Q_2 \end{bmatrix} &= \frac{1}{2} \begin{bmatrix} V_{2d} I_d + V_{2q} I_q \\ V_{2d} I_q - V_{2q} I_d \end{bmatrix} \\ &= K_P \begin{bmatrix} \sin\psi - \dfrac{1}{F_x Q_{L0}} \left(\dfrac{1}{M} - \cos\psi \right) \\ -\left(\dfrac{1}{M} - \cos\psi \right) - \dfrac{\sin\psi}{F_x Q_{L0}} \end{bmatrix} \end{aligned} \tag{5}$$

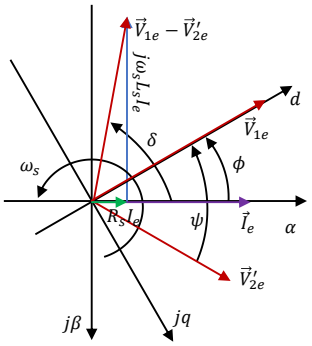

Fig. 3: Vector diagram.

where $K_P = \dfrac{8n}{\pi^2} \times \dfrac{V_1 V_2}{R_s} \times \dfrac{F_x Q_{L0}}{1 + F_x^2 Q_{L0}^2}$.

The term *active power* expresses the power component which is really transferred between the two terminal, and the term *reactive power* describes the circulating power component within the inverters. This reactive power contributes only to the conduction and copper dissipations of the converter [10]–[12]. Therefore, it should be depressed to reduce power losses and to improve the system efficiency.

Since the d-axis is intentionally aligned to $\vec{V}_1$, the quadrature voltage component V_{1q} equals to 0. Because of the high switching frequency, the voltage V_1 can be assumed as constant in one cycle. From (4), the active power P_1 is proportional to the direct current component I_d, meanwhile the reactive power Q_1 is proportional to the quadrature current component I_q. If I_d and I_q can be regulated individually, the active and reactive power at terminal 1 are completely controlled.

III. Proposal

A. Observer Design

From the primary referred equivalent circuit depicted in Fig. 2, the vector diagram expressed in Fig. 3 and the Kirchhoff Law, the small signal space state model (6) of the converter can be derived by linearizing around the operation point described by (1), (2) and (3). Note that, in the model (6), the variation of terminal voltages in one sampling cycle is neglected.

$$\frac{d}{dt}\boldsymbol{x} = \boldsymbol{A}\boldsymbol{x} + \boldsymbol{B}\boldsymbol{u} \tag{6}$$

where $\boldsymbol{A} = \begin{bmatrix} -\dfrac{R_s}{L_s} & -\Omega_s \\ \Omega_s & -\dfrac{R_s}{L_s} \end{bmatrix}$, $\boldsymbol{x} = \begin{bmatrix} \hat{i}_d(t) \\ \hat{i}_q(t) \end{bmatrix}$, $\boldsymbol{u} = \begin{bmatrix} \hat{f}_x \\ \hat{\psi} \end{bmatrix}$, $\boldsymbol{B} = \begin{bmatrix} -\Omega_s I_q & \dfrac{4n}{\pi L_s} V_2 \sin\psi \\ \Omega_s I_d & -\dfrac{4n}{\pi L_s} V_2 \cos\psi \end{bmatrix}$, $\hat{i}_d$, $\hat{i}_q$, $\hat{f}_x$ and $\hat{\psi}$ are the small signals of the corresponding quantities.

In order to closed-loop control of $i_d(t)$ and $i_q(t)$ separately, the two current components must be available to be fed-back. By using a suitable transducer, one can measure the transferred current, however, $i_d(t)$ and $i_q(t)$ are unmeasurable. Note that,

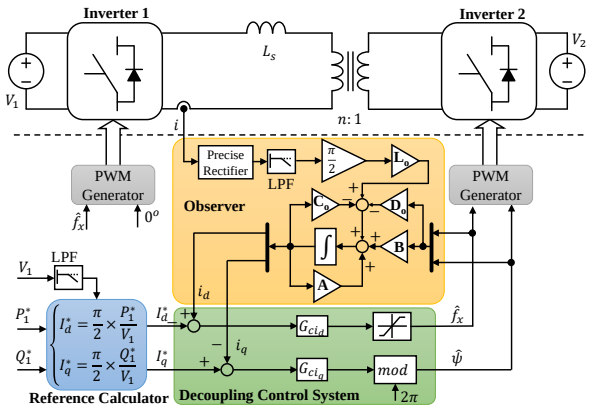

Fig. 4: Proposed control system diagram.

TABLE I: System Parameters.

Parameter	Symbol	Value	Unit
Port voltage	V_1	50	V
Port voltage	V_2	50	V
Trans. ratio	n	20:20	
Total inductance	L_s	25.38	μH
Total resistance	R_s	45.71	mΩ
Power electronic device	S_{1-4} T_{1-4}	CSD19536KCS	MOSFET
ON resistance	R_{DS}	2.3	mΩ
Nom. switching frequency	f_s	20	kHz
Nom. phase shift	ψ	25	deg
Sampling time	T_z	20	μs

the amplitude of the fundamental current component can be approximated by (7), where $i_{rec,avg}(t)$ is the average absolute value of the transferred current and it can be measured without difficulty by using a precise rectifier following by a low pass filter. Let $i_m(t)$ be the output signal of the system model, an observer can be designed to estimate $i_d(t)$ and $i_q(t)$ in real-time since the converter model has been specified. The observer model is given by (8).

$$i_m(t) = \sqrt{i_d^2(t) + i_q^2(t)} \approx \frac{\pi}{2} i_{rec,avg}(t) \tag{7}$$

$$\begin{cases} \frac{d}{dt}\boldsymbol{x} &= \boldsymbol{Ax} + \boldsymbol{Bu} + \boldsymbol{L_o}\left(i_m - \hat{i}_m\right) \\ \hat{i}_m &= \boldsymbol{C_o x} + \boldsymbol{D_o u} \end{cases} \tag{8}$$

where $\boldsymbol{C_o} = \left[\frac{I_d}{\sqrt{I_d^2 + I_q^2}} \quad \frac{I_q}{\sqrt{I_d^2 + I_q^2}}\right]$, $\boldsymbol{D_o} = \begin{bmatrix}0 & 0\end{bmatrix}$, $\hat{i}_m$ is the estimated amplitude of the fundamental component of the transferred current, and $\boldsymbol{L_o}$ is the observer gain matrix achieved by assigning the observer eigenvalues for the characteristic equation becomes the Butterworth polynomial (9). The crossover frequency ω_b is chosen as two to six times greater than the poles of (6) [13].

$$\det\left(s\boldsymbol{I} - \boldsymbol{A} + \boldsymbol{L_o C_o}\right) = 1 + \frac{s}{0.707\omega_b} + \frac{s^2}{\omega_b^2} \tag{9}$$

B. Decoupling Controller Design

In order to design two current controllers, a new system model expressed by (10) is built with the output signals are $i_d(t)$ and $i_q(t)$:

$$\begin{cases} \frac{d}{dt}\boldsymbol{x} &= \boldsymbol{Ax} + \boldsymbol{Bu} \\ \boldsymbol{y} &= \boldsymbol{Cx} + \boldsymbol{Du} \end{cases} \tag{10}$$

where $\boldsymbol{C} = \begin{bmatrix}1 & 0\\ 0 & 1\end{bmatrix}$, $\boldsymbol{D} = \begin{bmatrix}0 & 0\\ 0 & 0\end{bmatrix}$, $\boldsymbol{y} = \begin{bmatrix}\hat{i}_d(t)\\ \hat{i}_q(t)\end{bmatrix}$.

A laboratory-scaled-250W DAB converter is built to validate the proposed control strategy. Its parameters is given in Table I. Substitute parameters into the model (10), the relative gain array [14] can be calculated as (11):

$$\boldsymbol{RGA} = \begin{bmatrix}\lambda_{df} & \lambda_{d\psi}\\ \lambda_{qf} & \lambda_{q\psi}\end{bmatrix} = \begin{bmatrix}1.6950 & -0.6950\\ -0.6950 & 1.6950\end{bmatrix} \tag{11}$$

Since $\lambda_{d\psi}$ and λ_{qf} are negative, if i_d is paired with ψ and i_q is coupled with f_x, the system is unstable. Therefore, the f_x will be manipulate to regulate i_d, meanwhile ψ is controlled to regulate i_q. The control system diagram is illustrated in Fig. 4. A reference calculator basing on (4) is employed to generate current commands for the decoupling control system. Two simple PI controllers G_{cid} and G_{ciq} are designed for closed-loop control of i_d and i_q, respectively.

IV. Simulation and Experiment Results

Fig. 5 indicates the diagram of the experiment system. The DC input of the two inverters are connected to each other and to the output of a programmable DC power supply which is set at 50 V constantly. By using this configuration, the power source supplies only the dissipation. Two voltage transducers LEM LV25-P to measure the instantaneous DC voltage are reserved for future application. Two DC current clamps Hioki CT9691 are employed to measure the dissipated and the input currents of inverter 1. The transferred current is measured by using a current transducer LEM LN25-NP before leading to an external precise rectifier. PWM signals are generated from a TI-TMS320F28335 control card. The input parameters for the modulation, F_x and ψ, are provided from a dSPACE 1103 hardware-in-the-loop platform. The control system designed above is discretized with the sample time of 20 μs. By choosing $\omega_b = 50 \times \omega_s$, the observer gain matrix $\boldsymbol{L_o}$ in the discrete domain can be calculated using the Ackerman method [13]:

$$\boldsymbol{L_o} = \begin{bmatrix}2.2645 & -1.1033\end{bmatrix}^T \tag{12}$$

In order to evaluate the validity of the observer, both average absolute current and the load angle ϕ, $\phi = \arctan\frac{I_q}{I_d}$, are considered. In experiment, ϕ is determined by measuring the time difference between the zero crossing points of the transferred current and the primary voltage of the transformer.

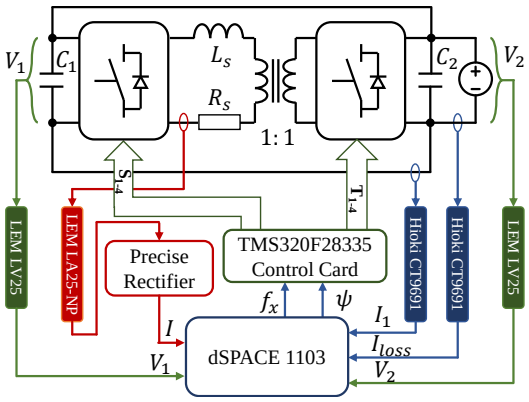

Fig. 5: Experiment system.

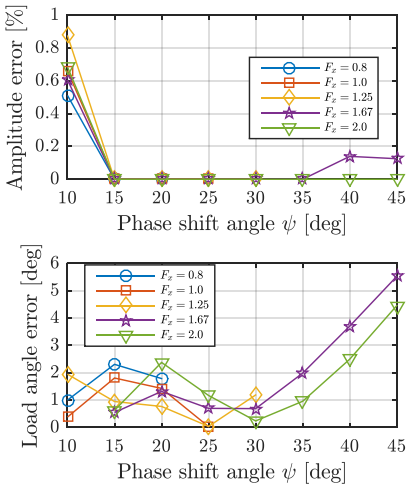

Fig. 6: Observer Performance.

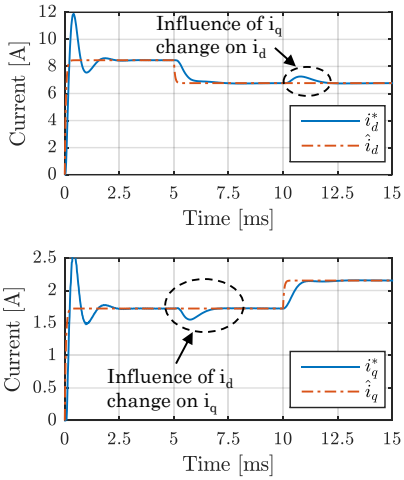

Fig. 7: Dynamic Response.

The frequency modulation factor f_x and bridge shift angle ψ are varied for power ranging from 50 W to 250 W.

The comparison results between the observed current amplitude and load angle with the measured ones are shown in Fig. 6. The amplitude error is almost zero for all examined value of f_x and ψ. The load angle error is zero at the nominal condition ($f_x = 1, \psi = 25^o$). However, as the operation changes far from the nominal point, the ψ error increases. This is comprehensible since the observer model is achieved by linearizing around the nominal operation point.

The simulation dynamic response demonstrated in Fig. 7 shows the performance of the decoupling control system. At first, the current reference is set at the nominal condition. At 5 ms the reference i_d^* drops 25%, and at 10 ms, the reference i_q^* steps up 25%. Due to the decoupling is accomplished by input-output pairing without any interaction compensation, the step change in either i_d or i_q affects the others. The current responses are stable after 2.5 ms since the reference changes.

V. Conclusion

This paper focus on the dynamic control for DAB converter. The two major contributions of this paper, which are confirmed by simulation and experiment, are as followed:

- An observer is designed in order to estimate the instantaneous i_d and i_q since it is impossible to measure them directly. This method requires only the average absolute value of the transferred current, which can be measured easily by a current transducer. Since the average absolute value is DC, the control system does not require a very high sampling speed.
- A decoupling control system of direct and quadrature current components, i_d and i_q has been developed. Because both i_d and i_q are DC quantities, there will be no errors at the steady state. Therefore, the active and reactive power can be managed individually. This allow us to manage Q_1 at a low amplitude to limit the circulating current while setting P_1 at the transmission demand.

References

[1] De Doncker. R. W. A. A., Divan. D. M., Kheraluwala. M. H., "A three-phase soft-switched high-power-density DC/DC converter for high-power applications," *IEEE Transaction on Industry Applications*, vol.27, no.1, pp.63-73, Jan/Feb 1991.

[2] H. Qin and J. W. Kimball , "Closed-loop control of DC-DC dual-active-bridge converters driving single-phase inverters" , *IEEE Trans. Power Electron.* , vol. 29 , no. 2 , pp.1006 -1017 , 2014.

[3] F. Krismer, and J. W. Kolar "Accurate small-signal model for the digital control of an automotive bidirectional dual active bridge", *IEEE Trans. Power Electron.*, vol. 24, no. 12, pp.2756-2768, 2009.

[4] R.T. Naayagi, A.J. Forsyth and R. Shuttleworth "High-power bidirectional DC-DC converter for aerospace applications", *IEEE Transactions on Power Electronics,* vol. 27, no. 11, pp.4366-4379, 2012.

[5] T. Zhao, G. Wang, S. Bhattacharya and A. Q. Huang , "Voltage and power balance control for a cascaded H-bridge converter-based solid-state transformer" , *IEEE Trans. Power Electron.* , vol. 28 , no. 4 , pp.1523 -1532 , 2013.

[6] D. Segaran , D. G. Holmes and B. P. McGrath , "Enhanced load step response for a bidirectional DC-DC converter" , *IEEE Trans. Power Electron.* , vol. 28 , no. 1 , pp.371 -379 , 2013.

[7] S. P. Engel, N. Soltau, H. Stagge and R. W. De Doncker , "Improved instantaneous current control for high-power three-phase dual-active bridge DC-DC converters" , *IEEE Trans. Power Electron.* , vol. 29 , no. 8 , pp.4067 -4077 , 2014.

[8] A. Tripathi , "Design Considerations of a 15kV SiC IGBT based medium-voltage high-frequency isolated DC-DC converter" , IEEE Trans. Ind. Applicat. , vol. 51 , no. 4 , 2015.

[9] M. Ciobotaru, R. Teodorescu, and F. Blaabjerg, "A new single-phase PLL structure based on second order generalized integrator," in *Proc. 37th IEEE PESC,* Jun. 2006, pp. 1-6

[10] N. D. Dinh, N. D. Tuyen, G. Fujita , T. Funabashi , "Dual-active-bridge series resonant converter: A new control strategy using phase-shifting combined frequency modulation," in *Proc. IEEE ECCE,* 20-24 Sept. 2015, pp.1215-1222.

[11] H. Bai, Z. Nie, and C. Mi, "Experimental comparision of traditional phase-shift, dual-phase-shift, and model-based control of isolated bidirectional dc-dc converters," *IEEE Trans. Power Electron.,* vol. 25, no. 6, pp. 1444-1449, Jun. 2010.

[12] M. Kim, M. Rosekeit, S. K. Sul, and D. Doncker, A dual-phase-shift control strategy for dual-active-bridge DCDC converter in wide voltage range, in *Proc. IEEE ECCE,* 2011, pp. 364371.

[13] G. F. Franklin, J. D. Powell, and M. Workman, *Digital Control of Dynamic Systems, 3rd Edition* Menlo Park, CA, USA: Addison-Wesley, 1997.

[14] Mahoney, D.P., Svrcek, W.Y., and B.R. Young, *A Real-Time Approach to Process Control, 2nd Edition,* John Wiley & Sons, Ltd., 2006.